COST OPTIMIZED DESIGN OF HIGH POWER LINACS

M. Eshraqi*
European Spallation Source, Lund, Sweden

Abstract

The research accelerators are growing in energy and power which translates to an increase in their cost, and also size when the conventional acceleration techniques are used. On the other hand, handling megawatts of power requires a design that is robust and respects the known criteria in beam physics to avoid losses in excess of one part in a million. Traditionally cost increases with power and quality of the accelerator and beam. In this paper, using the ESS linac as an example, this tradition is challenged and ways to reduce the cost while neither quality nor power is compromised are presented.

INTRODUCTION

The applications of the hadron linacs are becoming more and more diverse, from the very low power medical accelerators to the high power irradiation and spallation accelerators. Even when these linacs are used as injectors to rings, their power, complexity and cost is a considerable percentage of the total project cost [1]. While some of the design rules of high current linacs are irrelevant to low current accelerators, there are still several similarities in their design, architecture and optimization. The output energy and power of each of these accelerators is imposed to the design team through its goals and applications. Having a defined, limited budget, the linac should be redesigned and optimized several times to meet the goals, and all these should happen considering the fixed dates in the project. The risk factor should be added as another dimension to this triangle of scope, cost and schedule. While no one intends to take a higher risk, the constraints defining the base of this pyramid tend to push the risk higher and cut the margins. During the design and optimization one should consider reasonable mitigation schemes for these risks that are cost and schedule neutral. The goal of this paper is to share the experiences gained in the design and optimization of the ESS linac, specially those acquired during cost scrubbing.

HADRON LINACS

Some examples of recent hadron accelerators and their application are listed below.
European Spallation Source [2] is a spallation neutron source which produces neutrons through bombardment of neutron rich nuclei with high energy protons. The high flux of moderated, slow, neutrons is used to study the structure of e.g. biological substances. The Spallation Neutron Source, SNS [3] in Oak Ridge, US, uses a 1 MW superconducting linear accelerator as the main accelerator. The aging research reactors and the public resistance against new research nuclear reactors plus the pulsed structure of neutron flux out of spallation sources has made them even more attractive in recent years [3–5].

Neutrino beams [6] are produced using an intense beam of protons to create pions that upon decay produce muons and muon neutrinos as secondary particles. The oscillation of these muon neutrinos into other types of neutrinos will be detected at a detector far from the generation point to determine parameters that determine these oscillations. On a recent staged proposal, the muons could be captured, cooled and accelerated in a muon decay ring for a neutrino factory that could later be extended up to a muon collider [7].

Accelerator driven systems [8, 9] also called accelerator driven subcritical nuclear reactors or hybrid reactors as well as transmutation facilities [10] are being designed to produce cleaner and safer energy and transmute the long lived nuclear waste to short lived waste. Both of these applications need a multi-megawatt class accelerator in the GeV range. However, the fail/trip rate of these accelerators is orders of magnitude tighter than the existing accelerators. Though technically these machines are not insuperable, they are not yet economically very attractive, reducing the accelerators' construction and operation cost might affect that balance.

RULES OF THUMB ON LINAC DESIGN

When designing a high power hadron linac, one should consider few guidelines. The zero current phase advance per focusing period should not exceed 90° in any of the transverse or longitudinal planes. Having a zero current phase advance per focusing period above $\sigma_0 > 90°$ would cause envelope instabilities even at low beam currents [11]. The second important parameter is the average zero current phase advance, $k_0^2 \propto F$, where F is the external force on the beam. Having a smooth phase advance along the linac guarantees that the space charge equilibrium within the beam will not be altered abruptly at the transitions. Such abrupt changes in the focusing channel, either transverse of longitudinal, could increase the emittance [12] and depopulate the core of the beam.
For high intensity accelerators the tune depression (η), the ratio of phase advance with current (σ) to zero current

* mohammad.eshraqi@esss.se

ISBN 978-3-95450-142-7

phase advance (σ_0), is the figure of merit on how sensitive is the design to the space charge forces. There are numerous studies (e.g. [13, 14] and references therein) discussing this issue. It is universally agreed that a design with higher tune depression value – weaker space charge effect – would result in less halo formation and consequently less losses. For example Lagniel [13, 15] proposes to keep the tune depression above 0.4 to limit the number of mismatch resonances in the linac to two.
There are other recommendations for linac design such as constraining the ratios of phase advances to certain limits to avoid emittance exchange [16]. One can refer to [17] for a review of beam instabilities in ion linacs.

COST CONTRIBUTORS

There are already few papers on cost optimization of the hadron linacs [1, 18–20]. This paper looks at the cost contributors and their optimization possibilities. The scope of the project could define the energy, the power, or both of them as parameters of the linac. Assuming a defined power, that is more general, the total power is defined as:

$$P_b = I_b \cdot W_{linac}, \tag{1}$$

where P_b is the beam power, I_b the average beam current, and W_{linac} the linac final energy that could be written down as:

$$W_{linac} = q \sum_i k E_{acc_i}\, T_i\, L_i\, \cos(\phi_i), \tag{2}$$

where E_{acc_i}, T_i, L_i, ϕ_i, k and q are the max accelerating gradient, transit time factor, length, synchronous phase in i^{th} cavity, ratio of the applied accelerating field to the maximum accelerating field and charge of the particles respectively. Some of these parameters are functions of other parameters.

$$L_i = M_{cell_i} \cdot \frac{\beta_{g_i} \lambda_i}{n_i}, \tag{3}$$

the length of a cavity is a function of the number of cells M_{cell_i}, geometric beta of the cavity β_{g_i}, wavelength λ_i and mode of acceleration n_i.
The electric field in the cavities, specially for superconducting cavities, to be used during the design phase may not be known. One can use the data from the measurements in other facilities and make an educated guess for the linac design. Figure 1 shows the ratio of the peak surface field to the accelerating field of the cavities vs. their geometric betas. One can find different analytic expressions to interpolate between the points. The blue line in Fig. 1 is plotted using

$$\frac{E_{peak}}{E_{acc}} = \frac{1}{1.97/\beta_g + 1.22 \cdot \beta_g - 1}, \tag{4}$$

with E_{peak} usually in the range of 35 to 50 MV/m. One can therefore write the E_{acc_i} in Eq. 2 as a function of β_g and E_{peak} (f_{acc}),

$$E_{acc_i} = E_{peak} \cdot f_{acc}(\beta_g). \tag{5}$$

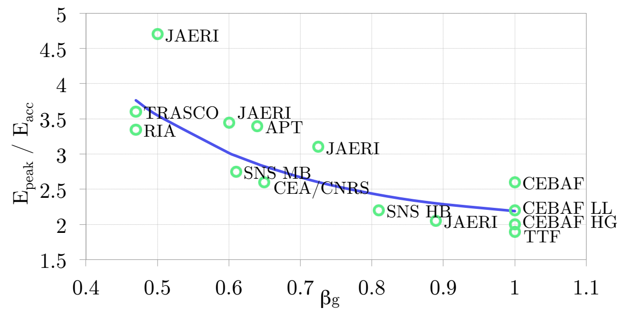

Figure 1: E_{peak}/E_{acc} as a function of geometric beta [21].

The average current of the beam could be written down as:

$$I_b = I_{max} \cdot f_{pulse} \cdot L_{pulse} = I_{max} \cdot d.c., \tag{6}$$

where I_{max}, f_{pulse}, L_{pulse} and $d.c.$ are respectively the peak current within the pulse, repetition rate of the linac, length of pulse and the duty factor of the linac.
The equations 2 to 6 could be substituted in Eq. 1 resulting in:

$$P_b = q \cdot I_{max} \cdot d.c. \cdot k \cdot E_{peak} \cdot \sum_i f_{acc}(\beta_g)\, T_i\, M_{cell_i} \cdot \frac{\beta_{g_i} \lambda_i}{n_i}\, \cos(\phi_i). \tag{7}$$

From Eq. 7 one can see that the free parameters are E_{peak}, I_{max}, $d.c.$, β_g, T, ϕ_s, M_{cell}, λ and k. Almost all linacs are built of different sections and another important parameter, not explicitly visible in this equation, is the transition energies between the sections. Another hidden parameter is the number of cavities per focusing period.

For example for the ESS SCL, there were 11 parameters to optimize at the hardware level: three β_gs, three cell numbers per cavity, three cavities per period for the spoke, medium and high β sections and two transition energies from spoke to medium β and medium to high β section [22].
Figure 2 shows the transit time factor as a function of geometric beta for the ESS elliptical cavities (solid lines) and in case the geometric beta is changed by ± 0.02 (dashed lines in the same figure). Choosing the right transition energy and the right geometric beta improves the average transit time factor, and therefore the acceleration efficiency of the linac.

Choosing the transition energies between the normal conducting structures and from normal conducting to superconducting should be considered too. For example in the ESS linac, the transition energy from Radio Frequency Quadrupole, RFQ, to Drift Tube Linac, DTL, was increased for several reasons: the accelerating efficiency of the DTL increases very rapidly with energy at low energies, higher injection energy to DTL results in longer DTL cells that are easier to manufacture, longer drift tubes provide larger space for permanent magnet quadrupoles, PMQs, these longer magnets can have a lower gradient while the

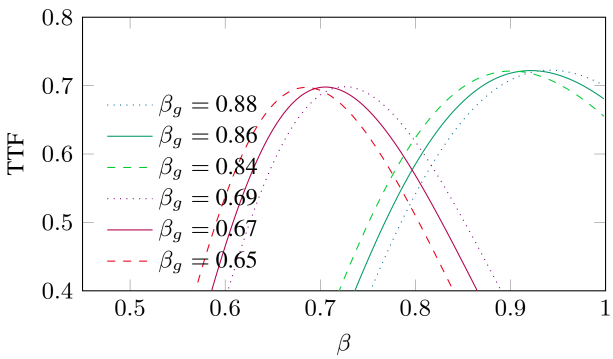

Figure 2: Transit time factor as a function of particle β for different geometric betas. The red series have six cells and the green series are five cell elliptical cavities.

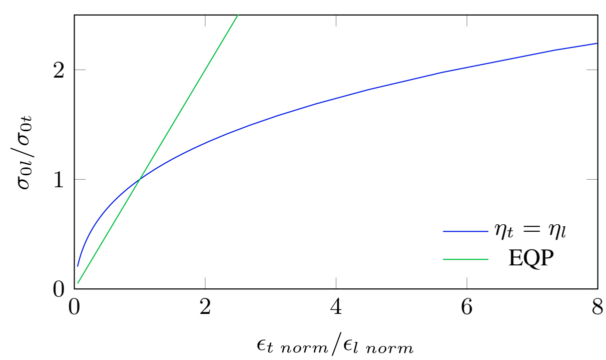

Figure 3: Zero current phase advance ratio as a function of the normalized emittance ratio to satisfy $\eta_t = \eta_l$.

integrated gradient stays the same, and finally increased gap size plus lower magnetic field at the surface of the drift tubes reduces the spark rate at the first gaps [23].

Transition energy from normal conducting to superconducting linac changes the balance between ohmic losses on the copper cavity surface vs. the static heat load on the cryo system. Considering only the power consumption, the higher the duty cycle, the lower should be the transition energy. To gain the maximum acceleration efficiency this transition should happen when the accelerating efficiency of the normal conducting linac reaches that of the following sc linac.

The duty factor of the ESS linac is a requirement from the neutron instruments and could not be played with. The frequency of the linac, and therefore λ, is usually chosen by looking at the available power sources and synergies with collaborating labs.

BEAM DYNAMICS

The rules of thumb on linac design has already been covered. Minor adjustments to the linac design could not only reduce the cost of the linac, they can as well improve the beam dynamics performance of the linac. Two of these adjustments employed in the latest design of the ESS linac are diverting from an equi-partition design and changing how the frequency jump is handled at the transition.

Equi-tune Depression vs. Equipartition

As the non-linear space charge forces are the main cause of halo growth, reducing their effect, in all the three planes, should be the goal. It is shown [15] that a design where the ratio of phase advances vs. the ratio of emittances follows the curve in Fig. 3 results in a linac with equal tune depressions, η, in all planes. They also make shorter linacs with respect to equipartition designs for beams with longitudinal to transverse emittance ratio of grater than one. If the aspect ratio of the beam is close to unity even an equipartition design would keep the tune depressions almost equal, but one does not gain anything by that choice.

Synchronous Phase

There are already several methods to handle the frequency jump in ion linacs [24], but these methods either use a local bunch rotation that violates the average phase advance continuity or vary the downstream structure settings to accept the beam. One of the main goals in each transition in a linac is to improve the efficiency of the structure, this is partly achieved by using structures that have a higher accelerating gradient as the beam energy increases. Reducing the gradients and lowering the synchronous phase of the downstream structure to achieve a better matching goes against this main goal. At the ESS linac the phases of the upstream structure (that has an accelerating gradient of 9 MV/m) is lowered along the section to keep the average phase advance constant (and equal to that of the downstream structure) instead of lowering the gradients in the downstream one (that has an accelerating gradient of $\sim$ 17 MV/m). This reduces the phase spread of the beam at the transition to assure a lossless capture by the following structure with improved beam performance and acceleration efficiency. The synchronous phase using this method and the method proposed in [24] are plotted in Fig. 4.

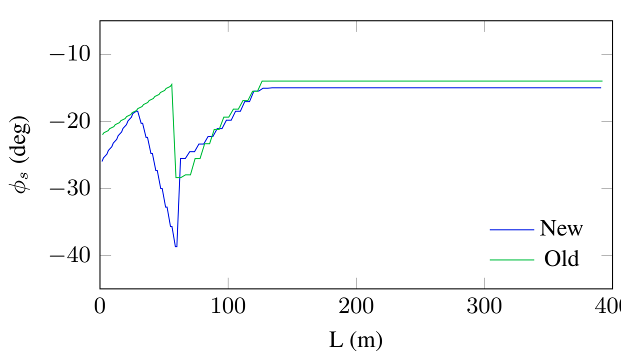

Figure 4: Synchronous phase along the sc linac for the new phase law and the old phase law [24].

The phase law is defined to keep the longitudinal phase advance constant (the flat blue line at $\sim$ 10 deg/m in Fig. 5). The longitudinal phase advance per meter could be written

ISBN 978-3-95450-142-7

as

$$k_{0l}^2 = \frac{2\pi q E_{acc} T \sin(-\phi_s)}{mc^2 \beta_s^3 \gamma_s^3 \lambda}, \quad (8)$$

and to keep this constant the synchronous phase should decrease as a function of energy

$$\sin(-\phi_s) = \frac{k_{0l}^2 mc^2 \beta_s^3 \gamma_s^3 \lambda}{2\pi q E_{acc} T} = const. \frac{\beta_s^3 \gamma_s^3}{E_{acc} T}, \quad (9)$$

where β_s and γ_s are the reduced velocity and mass of the synchronous particle. Using this method the average phase advance of the downstream structure need not be altered (the section of the green line with positive gradient in Fig. 5 between the two vertical red markers). Therefore the voltages (see Fig. 6) of the first cavities in the downstream structure could be as high as the phase advance per period does not exceed 90° for the synchronous particle. In reality since there is an energy spread in the beam some lower energy particles may see a higher phase advance than the synchronous particle and could have a phase advance of $> 90°$. To avoid this effect the phase advance of the synchronous particle is set to 83° per period.

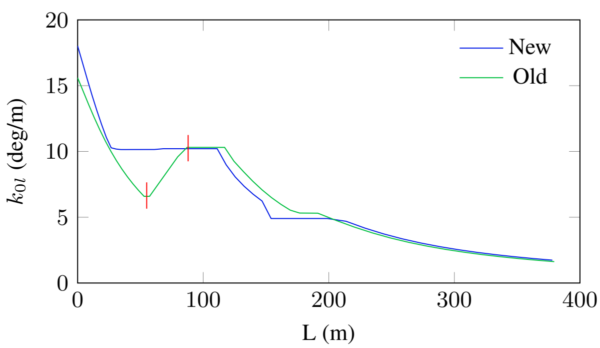

Figure 5: Zero current phase advance along the sc linac for the new phase law and the old phase law.

Having the cavities at a higher voltage results in a higher energy gain per cavity and therefore for a fixed final energy fewer cavities are needed. On top of that the power profile (see Fig. 7) for this scheme has a smaller dynamic range (4.1 vs. 13.3 between vertical dotted lines), improving the efficiency of the klystrons, reducing the integral of reflected power from cavities and therefore reducing the overall operational cost of the linac.

HARDWARE COST

It is reported that the rf power sources account for more than one third of the total linac cost [1, 25]. The cost of individual rf power sources as a function of their output power is modeled using existing vendor prices in [19], e.g. for klystrons

$$C(p) = C(p_0) \cdot (a_1 + a_2 \frac{p}{p_0}), \quad (10)$$

where $C(p)$ and $C(p)$ are the cost of klystron at the power level of p and p_0 and a_1 and a_2 are positive numbers. This

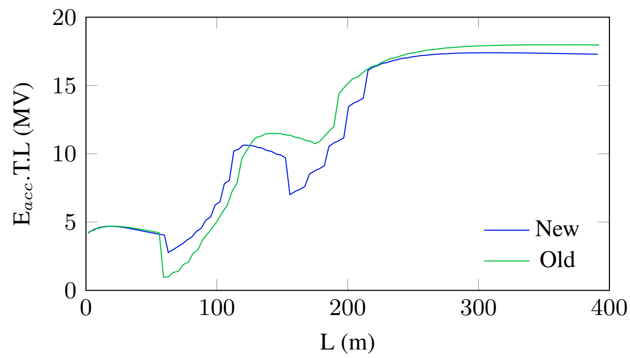

Figure 6: Voltage profile along the sc linac for the new phase law and the old phase law.

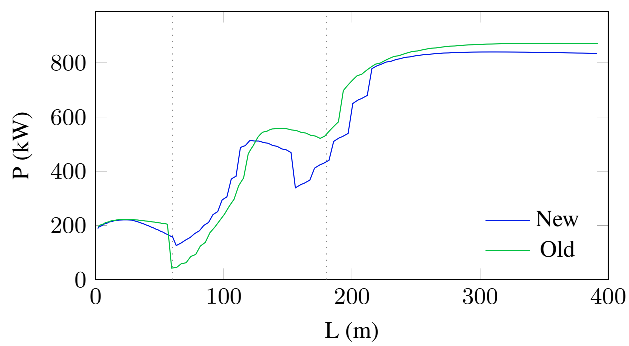

Figure 7: Power delivered to beam per cavity along the sc linac for the new phase law and the old phase law.

model recommends fewer, but more powerful rf sources. That is why the "new" frequency jump method could decrease the construction and the operation cost of the facility.

RISKS AND THEIR MITIGATION

The ESS linac took two major risks in going from the 2012 baseline [2] to the OPTIMUSPLUS lattice [26]. These two are the increased peak surface field in the SC cavities from 40 to 45 MV/m and increased beam current from 50 to 62.5 mA. The former affects the yield of the SC cavities, increasing the risk that a higher number of cavities are under performing, it affects the power required per cavity by 12.5% putting an extra burden on the rf couplers of the SC linac. The latter increases the risk of particle loss and activation, and also increases the power required per cavity by 25% affecting all the rf couplers. Since the energy and phase of the normal conducting linac can not be changed if couplers are power limited, for the NC linac instead of increasing the power per coupler the tanks were redesigned to stay at the safe value of 1.1 MW per coupler or lower.

There is a risk associated to pushing the boundaries of the state-of-the-art technology. One should consider adding margins or other mitigation means to the design to have the capability of handling these risks in the unlucky case they happen. For a linac the easiest solution is to provide enough space between the linac and the following structure, or the target, that would be filled with more accelerating structures. While this is true for a relativistic beam, the beam energy at the front end of the linac could be too low for good capture, acceleration efficiency and lossless transport in the following accelerating structures. The superconducting part of ESS linac is made using a uniform period length. The period length in the spoke section has been used as the "unit", where lengths of all the downstream structures is a multiple of this "unit" length. The medium β section which follows the spoke has twice the period length of spoke. This allows to replace one medium β period with two spoke periods, and increase the energy at the injection to the medium β. The period length in the high β section is identical to that of medium β and they could be easily swapped, and finally there is enough space at the end of the linac to accommodate more high β cryomodules.

The by-product of this mitigation scheme is reduced engineering on the design of medium β and high β cryomodules by using identical cryomodules. Not to have long drift spaces between the medium β cavities ($\beta_g = 0.67$), the number of cells is increased from 5 to 6. This additional cell makes the cavity length very close to that of high β ($\beta_g = 0.86$) keeping the coupler and tuner port locations on the cryomodules of these two cavity types the same.

CONCLUSION

What is stopping the new facilities to be built or upgraded, is not usually their technical complexity, but their cost. It was shown that the beam dynamics performance is not in conflict with cost reduction schemes of linacs if innovative beam physics design are applied. To reduce the construction, as well as the operation cost of the linac one can decrease the margins on the peak surface field of the cavities, but keep available enough space for a fall back solution to install the missing cavities.

ACKNOWLEDGMENT

This work would have been impossible without the early works of David McGinnis on cost scrubbing of the ESS linac as reported in [25].

REFERENCES

[1] J.-M. Lagniel, "Linac Architecture for High Power Proton Sources", *in proc.* LINAC 2000.

[2] S. Peggs, Ed. "Technical Design Report", eval.esss.lu.se/cgi-bin/public/DocDB/ShowDocument?docid=274

[3] J. Galambos, "SNS Performance and the Next Generation of High Power Accelerators", *in proc.* PAC 2009.

[4] Sh. Nagamiya, "Status of the J-PARC Facility", *in proc.* IPAC 2012.

[5] J. W. G. Thomason, et al., "Megawatt Upgrades for the ISIS Facility", *in proc.* HB 2008.

[6] T. R. Edgecock, et al., "High intensity neutrino oscillation facilities in Europe", Phys.Rev.ST-AB **16** 021002 (2013).

[7] J.-P. Delahaye, et al. "A Staged Muon Accelerator Facility for Neutrino and Collider Physics", IPAC 2014.

[8] J.-L. Biarrotte, "Accelerator reference design for the MYRRHA European ADS demonstrator", *in proc.* LINAC 2010.

[9] H. Nifenecker, et al., "Accelerator Driven Subcritical Reactors". (IoP, 2003).

[10] D, Barni "Status of the TRASCO Project", *in proc.* SRF 2001.

[11] J. Struckmeier, M. Reiser, "Theoretical Studies of Envelope Oscillations and Instabilities of Mismatched Intense Charged-Particle Beams in Periodic Focusing Channels", Part. Accel. 14, 227 (1984).

[12] T. P. Wangler, "RF Linear Accelerators", 2^{nd} Ed., (Wiley-VCH, 2008).

[13] J.-M. Lagniel. "Halos and Chaos in Space-Charge Dominated Beams", *in proc.* EPAC 1996.

[14] A. M. Sessler, "Collective Phenomena in Accelerators", *in proc.* LINAC 1972.

[15] M. Eshraqi, J-M, Lagniel, "On the Choice of Linac Parameters for Minimal Beam Losses", *in proc.* IPAC 2013.

[16] I. Hofmann, G. Franchetti, O. Boine-Frankenheim, J. Qiang, R. D. Ryne, Phys. Rev. ST. Accel. Beams, **6**, 024202 (2003).

[17] R. Duperrier, "Review of Instability Mechanisms in Ion Linacs", *in proc.* HB 2010.

[18] O. Brunner, S. Calatroni, E. Ciapala, M. Eshraqi, R. Garoby, F. Gerigk, A. Lombardi, R. Losito, V. Parma, C. Rossi, et al., "Assessment of the Basic Parameters of the CERN SPL", Phys.Rev.ST Accel.Beams **12** (2009) 070402.

[19] D. McGinnis, "New Design Approaches for High Intensity Superconducting Linacs - The New ESS Linac Design", *in proc.* IPAC 2014.

[20] T. Powers, "Optimization of SRF Linacs", *in proc.* SRF 2013.

[21] P. Pierini, "Analysis of gradients for proton linac", Gradients and Betas for ESS LINAC, Lund, September 2010, Sweden.

[22] M. Eshraqi, "Design and Optimization of the ESS Linac", *in proc.* IPAC 2011.

[23] A. Moretti, Z. Qian, J. Norem, Y. Torun, D. Li and M. Zisman, "Effects of high solenoidal magnetic fields on rf accelerating cavities", Phys.Rev.ST Accel.Beams **8**, 072001 (2005).

[24] R. Duperrier, N. Pichoff, and D. Uriot, "Frequency jump in an ion linac", Phys.Rev.ST Accel.Beams **10** (2007) 084201.

[25] D. McGinnis, "ESS Linac Design Options", eval.esss.lu.se/DocDB/0002/000273/001/ESSLinacDesignOptionsV3.pdf

[26] M. Eshraqi, "Beam physics design of the Optimus+ SC linac", eval.esss.lu.se/DocDB/0003/000309/003/OptimusPlus.pdf

ISBN 978-3-95450-142-7